The Effect of Carbon Nanotubes on Buckling Analysis of Embedded Oil Pipes Resting on Elastic Medium

H. Rahimipour

Pars oil & gas Co., Iran
E-mail: h.rahimipour@pogc.ir
*Corresponding author

A. Manouchehri far

Department of Mechanical Engineering,
Islamic Azad University, Khomeinishahr Branch, Iran
E-mail:manouchehri@iaukhsh.ac.ir

Abstract: In this study, the effect of carbon nanotube (CNT) on the buckling of the embedded sea lines is investigated. The sea lines are simulated with isotropic cylindrical shell subjected to thermal and mechanical loads. The sea line is reinforced by armchair CNTs, where characteristics of the equivalent nanocomposite being determined using Mori-Tanaka model. The elastic medium is modelled using Pasternak foundation. The governing equations are obtained based on strain-displacement, stress-strain and energy relations as well as Hamilton's principal. The influences of volume percent of CNTs in sea lines, geometrical parameters, elastic medium constants, temperature change and poison ratio on the buckling load of the system are investigated. Results indicate that the buckling load of the sea line increases with increasing volume percent of CNTs in sea lines. Hence, the CNTs are very useful as reinforcer for sea lines in order to increase the buckling load of the system.

Biographical notes: H. Rahimipour received his BSc degree from Islamic Azad University, Khomeinishahr Branch, in Isfahan, Iran. He then received his MSc degree from Islamic Azad University of Khomeinishahr in Isfahan, Iran, in 2010. His current research interests are nanotubes, and FGMs. **A. Manouchehrifard** is Assistant Professor of Mechanical Engineering at the Islamic Azad University of Khomeinishahr, Iran. He received his PhD from the university of Mosko, and MSc from Isfahan Universityand BSc in Mechanical engineering from Isfahan University, Iran. His current research interest focuses on vibration analysis, stability and elasticity.

1   INTRODUCTION

Composites offer advantageous characteristics of different materials with qualities that none of the constituents possess. Nanocomposites developed in recent years, have received much attention amongst researchers due to provision of new properties and exploiting unique synergism between materials. It has therefore found multiple applications in nanocomposites in a wide range of industries including oil and gas, petrochemical, wire and cable, electronics, automotive, and construction. CNTs used as the matrix reinforcers, apart from having high mechanical and chemical properties, present more resistant to oxidation than other conventional nano-reinforcers. Hence, they are used for high temperature applications [1-6].

In such applications, one of the most important issues is to accurately measure the vibration buckling characteristics of the systems. It is not surprising, therefore, that the study on this topic is constantly expanding in the past decades. Indeed, the buckling of pipes has been studied for more than six decades, both theoretically and experimentally. Elastic buckling of a thin cylindrical shell was analysed by Karam et al. [7]. Agrawal and Sobel studied the weight compressions of cylindrical shells with various stiffness under axial compression loadingand showed that honeycomb sandwiches offer a substantial weight advantage over a significant load range [8].

Hutchinson and He studied buckling of cylindrical shells with metal foam cores under similar load and obtained optimal outer shell thickness, core thickness and core density by minimizing the weight of geometrically perfect shell with a specified load carrying capacity [9]. Elastic stability of cylindrical shell with an elastic core under axial compression was investigated by GhorbanpourArani et al. using energy method [10]. They reported increased elastic stability and significant weight reduction of the cylindrical shells. Ye et al., however, investigated buckling of a thin-walled cylindrical shell with foam core of various thickness under axial compression and suggested that despite enhancing the resistance to buckling failure, increase in foam core thickness beyond 10% of the outer radius is inefficient due to extra cost and weight involved [11].

Active control of laminated cylindrical shells using fiber reinforced composites was studied by Ray and Reddy using Mori-Tanaka model. However, the reinforced materials used were CNTs [12]. Also, Mori–Tanaka models for the thermal conductivity of composites with interfacial resistance and particle size distributions were studied by Bohm and Nogales [13].

In order to investigate the effect of CNTs on the buckling of sea lines resting on Pasternak foundation, in this research, the CNTs are used as reinforcer for sea lines and characteristics of the equivalent nanocomposite being determined using Mori-Tanaka model. The governing equations are obtained based on strain-displacement, stress-strain and energy relations as well as Hamilton's principal. The effects of volume percent of CNTs in sea lines, geometrical parameters, elastic medium constants, temperature change and poison ratio on the buckling load of the sea line are discussed in details.

The organization of this paper is as follows. In section 2, the derivation of the motion equations is given. In section 3, the Mori-Tanaka model is reviewed. Energy method formulation is given in section 4. Solution procedure is also presented in section 5. In section 6, numerical results are given and discussed, and conclusions are given in the last section.

2   FORMULATION

An oil pipe of length L, which is described as a cylindrical shell embedded in elastic medium, is shown in Fig. 1.
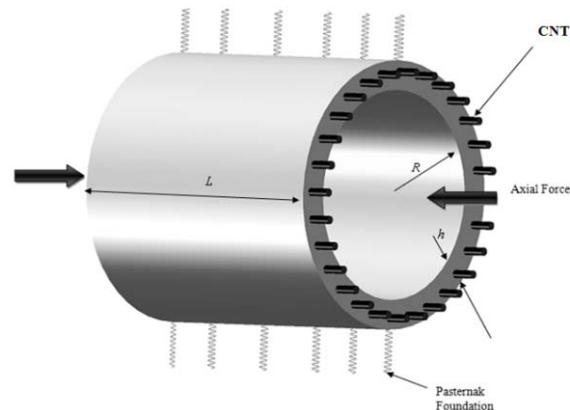
Fig. 1   **S**chematic view of sea line embedded in elastic medium

In order to calculate the middle-surface strain and curvatures, using Kirchhoff-Law assumptions, the displacement components of an arbitrary point may be written as [12]:

$$u(x,\theta,z,t) = u(x,\theta,t) - z\,\frac{\partial w(x,\theta,t)}{\partial x},$$

$$v(x,\theta,z,t) = v(x,\theta,t) - z\,\frac{\partial w(x,\theta,t)}{\partial \theta}, \qquad (1)$$

$$w(x,\theta,z,t) = w(x,\theta,t),$$

Where x and θ denote axial and circumferential direction of coordinate system, respectively, z is the distance from an arbitrary point to the middle surface

and R is the radius of the shell. Also u, v, w are the displacements of an arbitrary point of the shell in the axial, circumferential and radial directions, respectively. Using Donnell's theory, strains may be obtained by a combination of linear, nonlinear and curvature change terms as [12]:

$$\varepsilon_{xx} = \varepsilon_{xm} + zk_x,$$
$$\varepsilon_{\theta\theta} = \varepsilon_{\theta m} + zk_{\theta}, \qquad (2)$$
$$\gamma_{x\theta} = \gamma_{x\theta m} + zk_{x\theta}.$$

The mechanical strain components ε_{xx}, $\varepsilon_{\theta\theta}$, $\varepsilon_{x\theta}$ at an arbitrary point of the shell are related to the middle surface strains $\varepsilon_{x,0}$, $\varepsilon_{\theta,0}, \varepsilon_{x\theta,0}$ and change in the curvature and torsion of the middle surface k_x, k_{θ}, $k_{x\theta}$ as follows:

$$\begin{Bmatrix} \varepsilon_{xx} \\ \varepsilon_{\theta\theta} \\ \gamma_{x\theta} \end{Bmatrix}_{shell} = \begin{Bmatrix} \varepsilon_{xm} \\ \varepsilon_{\theta m} \\ \gamma_{x\theta m} \end{Bmatrix}_{L} + \begin{Bmatrix} \varepsilon_{xm} \\ \varepsilon_{\theta m} \\ \gamma_{x\theta m} \end{Bmatrix}_{NL} - z \begin{Bmatrix} k_x \\ k_{\theta} \\ k_{x\theta} \end{Bmatrix}$$

$$= \begin{pmatrix} \dfrac{\partial u}{\partial x} \\ \dfrac{\partial v}{R\,\partial\theta} + \dfrac{w}{R} \\ \dfrac{\partial u}{R\,\partial\theta} + \dfrac{\partial v}{\partial x} \end{pmatrix} + \begin{pmatrix} \dfrac{1}{2}\left(\dfrac{\partial w}{\partial x}\right)^2 \\ \dfrac{1}{2}\left(\dfrac{\partial w}{R\,\partial\theta}\right)^2 \\ \dfrac{\partial w}{\partial x}\dfrac{\partial w}{R\,\partial\theta} \end{pmatrix} - z\begin{pmatrix} \dfrac{\partial^2 w}{\partial x^2} \\ \dfrac{\partial^2 w}{R^2\partial\theta^2} \\ 2\dfrac{\partial^2 w}{R\partial x\partial\theta} \end{pmatrix}. \qquad (3)$$

The stress $(\sigma_{ijs}\ (i,j=x,\theta,z)$)-strain $(\varepsilon_{ijs}\ (i=x,\theta,z))$ relation for the cylindrical shell in general form can be written as [10].

$$\begin{bmatrix} \sigma_{xxs} \\ \sigma_{\theta\theta s} \\ \sigma_{zzs} \\ \sigma_{xzs} \\ \sigma_{\theta s} \\ \sigma_{x\theta s} \end{bmatrix} = \begin{bmatrix} C_{11} & C_{12} & C_{13} & 0 & 0 & 0 \\ C_{12} & C_{22} & C_{23} & 0 & 0 & 0 \\ C_{13} & C_{23} & C_{33} & 0 & 0 & 0 \\ 0 & 0 & 0 & C_{44} & 0 & 0 \\ 0 & 0 & 0 & 0 & C_{55} & 0 \\ 0 & 0 & 0 & 0 & 0 & C_{66} \end{bmatrix} \begin{bmatrix} \varepsilon_{xxs} - \alpha_{xxs}\Delta T \\ \varepsilon_{\theta\theta s} - \alpha_{s\theta\theta}\Delta T \\ \varepsilon_{zzs} - \alpha_{szz}\Delta T \\ \varepsilon_{xzs} \\ \varepsilon_{\theta s} \\ \varepsilon_{x\theta s} \end{bmatrix}, \qquad (4)$$

Where $C_{ij}\ (i,j=x,\theta,z)$, $\alpha_{kks}\ (k=x,\theta,z\ )$ and ΔT are elastic constants, thermal expansion coefficient and temperature difference, respectively. Using Eq. (3), the above relation can be expressed as:

$$\begin{bmatrix} \sigma_{xxs} \\ \sigma_{\theta\theta s} \\ \tau_{x\theta s} \end{bmatrix} = \begin{bmatrix} C_{11} & C_{12} & 0 \\ C_{21} & C_{22} & 0 \\ 0 & 0 & C_{66} \end{bmatrix} \begin{bmatrix} \varepsilon_{xxs} - \alpha_{xxs} \\ \varepsilon_{\theta\theta s} - \alpha_{\theta\theta s} \\ \gamma_{x\theta s} \end{bmatrix}, \qquad (5)$$

It should be noted that in Eq. (5), C_{ij} can be obtained using Mori-Tanaka model which is explained in next section.

3   MORI-TANAKA MODEL

In this section, the effective modulus of the composite shell reinforced by CNTs is developed. Different methods are available to estimate the overall properties of a composite [14]. Due to its simplicity and accuracy even at high volume fractions of the inclusions, the Mori-Tanaka method is employed in this section [15]. To begin with, the CNTs are assumed to be aligned and straight with uniformdispersion in the polymer. The matrix is assumed to be elastic and isotropic, with the Young's modulus E_m and the Poisson's ratio υ_m . The constitutive relations for a layer of the composite with the principal axes parallel to r,θ and z directions are [16]:

$$\begin{bmatrix} \sigma_{xxs} \\ \sigma_{\theta\theta s} \\ \sigma_{zzs} \\ \sigma_{xzs} \\ \sigma_{\theta zs} \\ \sigma_{x\theta s} \end{bmatrix} = \begin{bmatrix} k+M & l & k-M & 0 & 0 & 0 \\ l & N & l & 0 & 0 & 0 \\ k-M & l & k+M & 0 & 0 & 0 \\ 0 & 0 & 0 & p & 0 & 0 \\ 0 & 0 & 0 & 0 & M & 0 \\ 0 & 0 & 0 & 0 & 0 & p \end{bmatrix} \begin{bmatrix} \varepsilon_{xxs} \\ \varepsilon_{\theta\theta s} \\ \varepsilon_{zzs} \\ \varepsilon_{xzs} \\ \varepsilon_{\theta zs} \\ \varepsilon_{x\theta s} \end{bmatrix}, \qquad (6)$$

Where k, M, N, l, p are Hill's elastic moduli [16]; k is the plane-strain bulk modulus normal to the fiber direction, N is the uniaxial tension modulus in the fiber direction, l is the associated cross modulus, M and p are the shear moduli in planes normal and parallel to the fiber direction, respectively. According to the Mori-Tanaka method the stiffness coefficients are given by [16]:

$$k = \frac{E_m\{E_m c_m + 2k_r(1+v_m)[1+c_r(1-2v_m)]\}}{2(1+v_m)[E_m(1+c_r-2v_m)+2c_m k_r(1-v_m-2v_m^2)]}$$

$$l = \frac{E_m\{c_m v_m[E_m + 2k_r(1+v_m)] + 2c_r l_r(1-v_m^2)]\}}{(1+v_m)[E_m(1+c_r-2v_m)+2c_m k_r(1-v_m-2v_m^2)]}$$

$$n = \frac{E_m^2 c_m(1+c_r-c_m v_m)+2c_m c_r(k_r n_r - l_r^2)(1+v_m)^2(1-2v_m)}{(1+v_m)[E_m(1+c_r-2v_m)+2c_m k_r(1-v_m-2v_m^2)]}$$
$$+ \frac{E_m[2c_m^2 k_r(1-v_m)+c_r n_r(1+c_r-2v_m)-4c_m l_r v_m]}{E_m(1+c_r-2v_m)+2c_m k_r(1-v_m-2v_m^2)} \qquad (7)$$

$$p = \frac{E_m[E_m c_m + 2p_r(1+v_m)(1+c_r)]}{2(1+v_m)[E_m(1+c_r)+2c_m p_r(1+v_m)]}$$

$$m = \frac{E_m[E_m c_m + 2m_r(1+v_m)(3+c_r-4v_m)]}{2(1+v_m)\{E_m[c_m+4c_r(1-v_m)]+2c_m m_r(3-v_m-4v_m^2)\}}$$

Where C_m and C_r are the volume fractions of the matrix and the CNTs respectively, and kr, l_r, n_r, p_r, m_r are the Hills elastic modulus for the CNTs.

5   ENERGY METHOD

The total energy, V, consists of the potential energy U and W the virtual work due to external forces including, elastic medium is modeled using spring Winkler and shear Pasternak constants. The potential energy can be written as:

$$U_s = \int_{-\frac{h_s}{2}}^{\frac{h_s}{2}} \int_A \left(\sigma_{xxs}\left(\frac{\partial u}{\partial x} + 0.5\left(\frac{\partial w}{\partial x} \right)^2 - z\frac{\partial^2 w}{\partial x^2} \right) \right.$$

$$+ \sigma_{\theta\theta s}\left(\frac{\partial v}{R_s \partial\theta} + \frac{w}{R_s} + 0.5\left(\frac{\partial w}{R_s \partial\theta} \right)^2 - z\frac{\partial^2 w}{R_s^2 \partial\theta^2} \right) \tag{8}$$

$$\left. + \sigma_{x\theta s}\left(\frac{\partial u}{R_s \partial\theta} + \frac{\partial v}{\partial x} + \frac{\partial w}{R_s \partial\theta}\frac{\partial w}{\partial x} - 2z\frac{\partial^2 w}{R_s \partial\theta \partial x} \right) \right) dz\, dA$$

Where dA and dz are integral elements in surface and in thickness direction, respectively. The normal resultant force N_x and bending moment M_x can be expressed as [12]:

$$\begin{Bmatrix} N_{xs} \\ N_{\theta s} \\ N_{x\theta s} \end{Bmatrix} = \int_{-\frac{h}{2}}^{\frac{h}{2}} \begin{Bmatrix} \sigma_{xx} \\ \sigma_{\theta\theta} \\ \tau_{x\theta} \end{Bmatrix} dz = \begin{bmatrix} A_{11} & A_{12} & 0 \\ A_{12} & A_{22} & 0 \\ 0 & 0 & A_{66} \end{bmatrix} \begin{Bmatrix} \varepsilon_{xx} \\ \varepsilon_{\theta\theta} \\ \gamma_{x\theta} \end{Bmatrix}$$

$$- \begin{bmatrix} B_{11} & B_{12} & 0 \\ B_{12} & B_{22} & 0 \\ 0 & 0 & B_{66} \end{bmatrix} \begin{Bmatrix} k_x \\ k_\theta \\ k_{x\theta} \end{Bmatrix} - \begin{Bmatrix} N_x^T \\ N_\theta^T \\ 0 \end{Bmatrix}, \tag{9}$$

$$\begin{Bmatrix} M_x \\ M_\theta \\ M_{x\theta} \end{Bmatrix} = \int_{-\frac{h}{2}}^{\frac{h}{2}} \begin{Bmatrix} \sigma_x \\ \sigma_\theta \\ \tau_{x\theta} \end{Bmatrix} z\, dz = \begin{bmatrix} B_{11} & B_{12} & 0 \\ B_{12} & B_{22} & 0 \\ 0 & 0 & B_{66} \end{bmatrix} \begin{Bmatrix} \varepsilon_x \\ \varepsilon_\theta \\ \gamma_{x\theta} \end{Bmatrix}$$

$$- \begin{bmatrix} S_{11} & S_{12} & 0 \\ S_{12} & S_{22} & 0 \\ 0 & 0 & S_{66} \end{bmatrix} \begin{Bmatrix} k_x \\ k_\theta \\ k_{x\theta} \end{Bmatrix} - \begin{Bmatrix} M_x^T \\ M_\theta^T \\ 0 \end{Bmatrix}, \tag{10}$$

Where

$$\begin{pmatrix} \{ A_{ij}, \ B_{ij}, \ S_{ij} \} \\ \{ N_n^T, \ M_n^T, \ 0 \} \end{pmatrix} = \int_{-\frac{h}{2}}^{\frac{h}{2}} \begin{pmatrix} \{1, \ z, \ z^2\} \\ \{1, \ z, \ 0\} \end{pmatrix} \times \begin{pmatrix} \{C_{ij}\} \\ \{\alpha_n C_{ij}\} \end{pmatrix} dz \tag{11}$$

$$[i, j = 1,2,...6] \quad [n = x, \theta].$$

Using Eqs. (9)-(11), then Eq. (8) becomes:

$$U_s = \int_A \left[N_x\left(\frac{\partial u}{\partial x} + 0.5\left(\frac{\partial w}{\partial x} \right)^2 \right) - M_x\frac{\partial^2 w}{\partial x^2} \right.$$

$$+ N_\theta\left(\frac{\partial v}{R_s \partial\theta} + \frac{w}{R_s} + 0.5\left(\frac{\partial w}{R_s \partial\theta} \right)^2 \right) \tag{12}$$

$$- M_{\theta s}\frac{\partial^2 w}{R_s^2 \partial\theta^2} + N_{x\theta}\left(\frac{\partial u}{R_s \partial\theta} + \frac{\partial v}{\partial x} + \frac{\partial w}{R_s \partial\theta}\frac{\partial w}{\partial x} \right)$$

$$\left. - 2M_{x\theta s}\frac{\partial^2 w}{R_s \partial\theta \partial x} \right) dA$$

Where the normal resultant force and bending moment are:

$$N_x = \left(h_s C_{s11}\left(\frac{\partial u}{\partial x} + 0.5\left(\frac{\partial w}{\partial x} \right)^2 - \alpha_{sx}\Delta T \right) \right.$$

$$\left. + C_{s12}\left(\frac{\partial v}{R_s \partial\theta} + \frac{w}{R_s} + 0.5\left(\frac{\partial w}{R_s^2 \partial\theta} \right)^2 - \alpha_{s\theta}\Delta T \right) \right),$$

$$N_\theta = \left(h_s C_{s12}\left(\frac{\partial u}{\partial x} + 0.5\left(\frac{\partial w}{\partial x} \right)^2 - \alpha_{sx}\Delta T \right) \right. \tag{13}$$

$$\left. + C_{s22}\left(\frac{\partial v}{R_s \partial\theta} + \frac{w}{R_s} + 0.5\left(\frac{\partial w}{R_s^2 \partial\theta} \right)^2 - \alpha_{s\theta}\Delta T \right) \right),$$

$$N_{x\theta} = h_s\left(C_{s66}\left(\frac{\partial u}{R_s \partial\theta} + \frac{\partial v}{\partial x} + \frac{\partial w}{R_s \partial\theta}\frac{\partial w}{\partial x} \right) \right),$$

$$M_x = \frac{h_s^3}{12}\left(C_{s11}\left(-z\frac{\partial^2 w}{\partial x^2} \right) + C_{s12}\left(-z\frac{\partial^2 w}{R_s^2 \partial\theta^2} \right) \right), \tag{14}$$

$$M_\theta = \frac{h_s^3}{12}\left(C_{s12}\left(-z\frac{\partial^2 w}{\partial x^2}_x \right) + C_{s22}\left(-z\frac{\partial^2 w}{R_s^2 \partial\theta^2} \right) \right),$$

$$M_{x\theta} = \frac{h_s^3}{12}C_{s66}\left(-2z\frac{\partial^2 w}{R_s \partial\theta \partial x} \right)$$

The virtual work due to elastic medium can be expressed as:

$$W = -\int (F_e)w\, dA = -\int (K_W w - K_g\nabla^2 w)w\, dA, \tag{15}$$

Where K_w and K_g are Winkler and Pasternak modules, respectively. The governing equations of the sea lines embedded in an elastic medium can be derived from the Hamilton principle [12].

$$\int_{t_0}^{t_1} [\delta U - \delta W] = 0 \tag{16}$$

Substituting Eqs. (12) and (15) into Eq. (16), the governing equations can be written as:

$$\frac{\partial N_x}{\partial x} + \frac{\partial N_{x\theta}}{R\partial\theta} + P_x = 0 \tag{17}$$

$$\frac{\partial N_\theta}{R\partial\theta} + \frac{\partial N_{x\theta}}{\partial x} + P_\theta = 0 \tag{18}$$

$$\frac{\partial^2 M_x}{\partial x^2} + \frac{2\partial M_{x\theta}}{R\partial x\partial\theta} + \frac{\partial^2 M_\theta}{R^2\partial\theta^2} - \frac{N_\theta}{R} + N_x\frac{\partial^2 w}{\partial x^2} \tag{19}$$

$$+ N_\theta\frac{\partial^2 w}{R^2\partial\theta^2} + N_{x\theta}\frac{2\partial^2 w}{R\partial x\partial\theta} + P_z = 0.$$

Where P_x, P_θ, P_z are forces in axial, circumferential and radial directions, respectively.Substituting Eqs. (13) and (14) into Eqs. (17)-(19), the governing equations can be expressed and presented as in Appendix A.Introducing the following dimensionless quantities:

$$\gamma_s = \frac{h_s}{l}, \qquad \xi = \frac{x}{l}, \qquad \beta_s = \frac{h_s}{R_s},$$

$$\{\bar{u}, \bar{v}, \bar{w}\} = \frac{\{u, v, w\}}{h_s}, \quad \bar{C}_{kij} = \frac{C_{kij}}{C_{s11}}, \tag{20}$$

$$K_{wk} = \frac{h_s k_{wk}}{C_{s11}}, \qquad K_{gk} = \frac{k_{gk}}{h_s C_{s11}}, \bar{N}_x = \frac{N_x}{lC_{s11}}$$

The dimensionless governing equations can be expressed as:

$$\gamma_s^2\left(\frac{\partial^2\bar{u}}{\partial\xi^2} + \gamma_s\frac{\partial\bar{w}}{\partial\xi}\frac{\partial^2\bar{w}}{\partial\xi^2}\right) + \gamma_s\beta_s\bar{C}_{s12}\left(\begin{array}{c}\frac{\partial^2\bar{v}}{\partial\xi\partial\theta} + \frac{\partial\bar{w}}{\partial\xi}\\ + \beta_s\frac{\partial\bar{w}}{\partial\theta}\frac{\partial^2\bar{w}}{\partial\xi\partial\theta}\end{array}\right) \tag{21}$$

$$+\beta_s\bar{C}_{s66}\left(\beta_s\frac{\partial^2\bar{u}}{\partial\theta^2} + \gamma_s\frac{\partial^2\bar{v}}{\partial\xi\partial\theta} +\right.$$

$$\left.\beta_s\gamma_s\frac{\partial\bar{w}}{\partial\xi}\frac{\partial^2\bar{w}}{\partial\theta^2} + \gamma_s\frac{\partial\bar{w}}{\partial\xi} + \beta_s\gamma_s\frac{\partial\bar{w}}{\partial\theta}\frac{\partial^2\bar{w}}{\partial\xi\partial\theta}\right) = 0,$$

$$\beta_s\bar{C}_{s12}\left(\gamma_s\frac{\partial^2\bar{u}}{\partial\xi\partial\theta} + \gamma_s^2\frac{\partial\bar{w}}{\partial\xi}\frac{\partial^2\bar{w}}{\partial\xi\partial\theta}\right) + \beta_s^2\bar{C}_{s22}\left(\begin{array}{c}\frac{\partial^2\bar{v}}{\partial\theta^2} + \frac{\partial\bar{w}}{\partial\theta}\\ + \beta_s\frac{\partial\bar{w}}{\partial\theta}\frac{\partial^2\bar{w}}{\partial\theta^2}\end{array}\right) \tag{22}$$

$$+\gamma_s\bar{C}_{s66}\left(\begin{array}{c}\frac{\beta_s\frac{\partial^2\bar{u}}{\partial\xi\partial\theta} + \gamma_s\frac{\partial^2\bar{v}}{\partial\xi^2} +}{\frac{\beta_s\gamma_s\frac{\partial^2\bar{w}}{\partial\theta\partial\xi}\frac{\partial\bar{w}}{\partial\xi} + \beta_s\gamma_s\frac{\partial\bar{w}}{\partial\theta}\frac{\partial^2\bar{w}}{\partial\xi^2}}}\end{array}\right) = 0,$$

$$\frac{\gamma_s^2}{12}\left(-\gamma_s^2\frac{\partial^4\bar{w}}{\partial\xi^4} - 2\bar{C}_{s12}\beta_s^2\frac{\partial^4\bar{w}}{\partial\xi^2\partial\theta^2} - \beta_s^2\bar{C}_{s22}\frac{\partial^4\bar{w}}{\partial\theta^4}\right)$$

$$-\frac{\gamma_s^2\beta_s^2\bar{C}_{c66}}{3}\left(\frac{\partial^4\bar{w}}{\partial\xi^2\partial\theta^2}\right) - \gamma_s\beta_s\bar{C}_{s12}\left(\frac{\partial\bar{u}}{\partial\xi} + \frac{\gamma_s}{2}\left(\frac{\partial\bar{w}}{\partial\xi}\right)^2\right)$$

$$-\beta_s\bar{C}_{s22}\left(\frac{\partial\bar{v}}{\partial\theta} + \beta_s\bar{w} + \frac{\beta_s^2}{2}\left(\frac{\partial\bar{w}}{\partial\theta}\right)^2\right) \tag{23}$$

$$-\left(\beta_s^2\bar{C}_{s12}\alpha_{xs} + \beta_s^2\bar{C}_{s22}\alpha_{\theta s}\right)\frac{\partial^2\bar{w}}{\partial\theta^2}\Delta T$$

$$-\left(\gamma_s^2\alpha_{xs} + \gamma_s^2\bar{C}_{s12}\alpha_{\theta s}\right)\frac{\partial^2\bar{w}}{\partial\xi^2}\Delta T + \gamma_s\bar{N}_x\frac{\partial^2\bar{w}}{\partial\xi^2}$$

$$+K_{ws}\bar{w} - K_{gs}\left(\gamma_s\frac{\partial^2\bar{w}}{\partial\xi^2} + \beta_s\frac{\partial^2\bar{w}}{\partial\theta^2}\right) = 0$$

5   SOLUTION METHOD

As mentioned before, in the buckling of a sea line reinforced with CNTs, the boundary conditions defined for two circular ends of the shell are simply supported mechanical boundary conditions. For the mechanical one $u = v = w = w_{,xx} = 0$. The simply supported mechanical boundary condition is selected because in practice, simply supported ends could be achieved approximately by connecting the shell to thin end plates and rings. Hence, the three displacement mode shapes may be written as [10]:

$$u(x,\theta) = u_0\cos(\frac{m\pi x}{L})\cos(n\theta),$$

$$v(x,\theta) = v_0\sin(\frac{m\pi x}{L})\sin(n\theta), \tag{24}$$

$$w(x,\theta) = w_0\sin(\frac{m\pi x}{L})\cos(n\theta),$$

Where m and n are half axial and circumferential wave numbers, respectively. It should be noted that m is any positive number, while n is an integer. Finally, using Eq. (24), the governing equations considering linear terms can be written in matrix form as:

$$\begin{bmatrix}\left(-\gamma_s^2\frac{m^2\pi^2}{L^2} - \beta_s^2\bar{C}_{s66}n^2\right) & L_{12} & L_{13}\\ \left(\beta_s\bar{C}_{s12}\gamma_s\frac{mn\pi}{L} + \gamma_s\bar{C}_{s66}\beta_s\frac{mn\pi}{L}\right) & L_{22} & -n\\ \left(\gamma_s\beta_s\bar{C}_{s12}\frac{m\pi}{L}\right) & \left(-\beta_s\bar{C}_{s22}n\right) & L_{33}\end{bmatrix}\begin{bmatrix}u_0\\ v_0\\ w_0\end{bmatrix} \tag{25}$$

Where

$$L_{12} = \left(\gamma_s \beta_s \, \overline{C}_{s12} \, \frac{mn\pi}{L} + \beta_s \overline{C}_{s66} \gamma_s \, \frac{mn\pi}{L} \right),$$

$$L_{13} = \left(\gamma_s \beta_s \, \overline{C}_{s12} \, \frac{m\pi}{L} + \beta_s \overline{C}_{s66} \gamma_s \, \frac{m\pi}{L} \right),$$

$$L_{22} = \left(-\beta_s^2 \overline{C}_{s22} n^2 - \gamma_s \overline{C}_{s66} \gamma_s \, \frac{m^2\pi^2}{L^2} \right)$$

$$L_{33} = \left(\frac{\gamma_s^2}{12} \left(-\gamma_s^2 \, \frac{m^4\pi^4}{L^4} - 2\overline{C}_{s12}\beta_s^2 \, \frac{m^2\pi^2}{L^2} - \beta_s^2 \overline{C}_{s22} m^4 \right) \right.$$

$$\quad -\frac{\gamma_s^2 \beta_s^2 \overline{C}_{c66}}{3} \, \frac{m^2\pi^2}{L^2} - \beta_s^2 \overline{C}_{s22} + \left(\beta_s^2 \, \overline{C}_{s12} \alpha_{xs} + \beta_s^2 \, \overline{C}_{s22} \, \alpha_{\theta s} \right) n^2 \Delta T$$ (26)

$$\quad + \left(\gamma_s^2 \, \alpha_{xs} + \gamma_s^2 \overline{C}_{s12} \, \alpha_{\theta s} \right) \frac{m^2\pi^2}{L^2} \Delta T - \gamma \overline{N}_x \, \frac{m^2\pi^2}{L^2}$$

$$\quad \left. + K_{ws} - K_{gs} \left(-\gamma_s \, \frac{m^2\pi^2}{L^2} - \beta_s n^2 \right) \right).$$

In order to obtain a non-trivial solution, it is necessary to set the determinant of the coefficient matrix in Eq. (25) equal to zero to obtain the buckling load of the sea line.

6   NUMERICAL RESULTS

A simply supported pipe with $R_s = 813 \; mm$, $l = 93408 \; m$, $h_s = 22.2 \; mm$ can now be investigated using the proposed method. In the following subsections, based on the analytical method mentioned in section5, the buckling load of the sea line is obtained so that the effects of volume percent of CNTs in sea lines, geometrical parameters, elastic medium constants, temperature change and poison ratio on the buckling load of the system are studied and discussed in details.

Fig. 2 shows the dimensionless buckling load versus volume percent of CNTs in sea lines for different axial mode numbers. As can be seen, the dimensionless buckling load increases with increasing volume percent of CNTs. This is because increasing the volume percent of CNTs leads to a stiffer structure. It is also obvious that with increasing axial mode numbers, the dimensionless buckling load increases. The effect of temperature change on the dimensionless buckling load with respect to the volume percent of CNTs in sea lines is demonstrated in Fig. 3. It can be found that the dimensionless buckling load is decreased with increasing temperature change. The reason is that the equivalent stiffness in eigenvalue problem decreases with increasing temperature gradient. Furthermore, the effect of temperature change on the dimensionless buckling load becomes more remarkable at higher volume percent of CNTs.
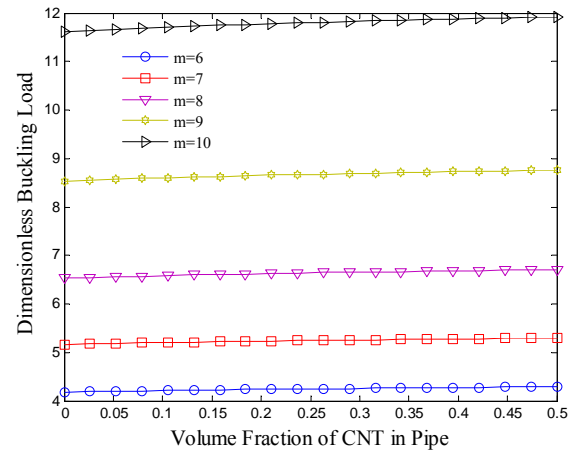

Fig. 2   The effect of axial mode number on the dimensionless buckling load versus volume percent of CNTs in sea lines
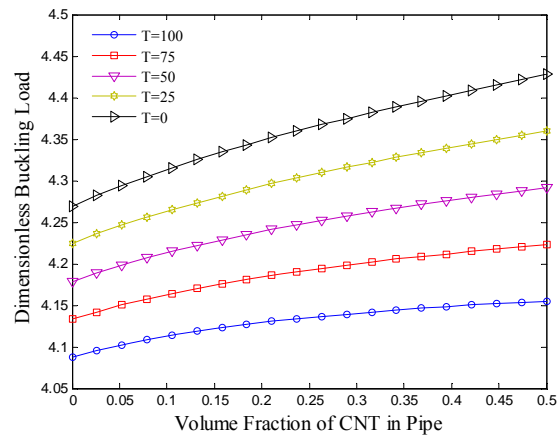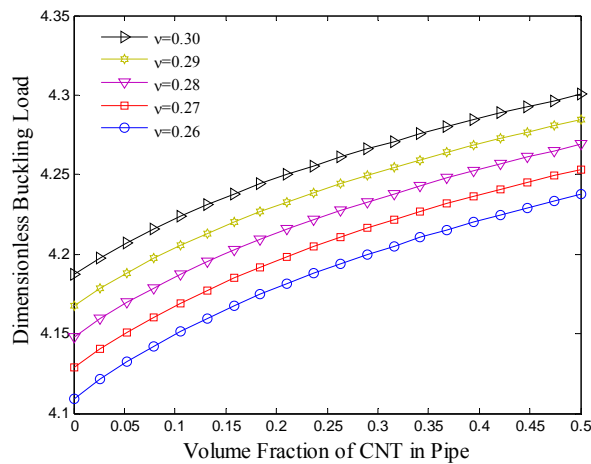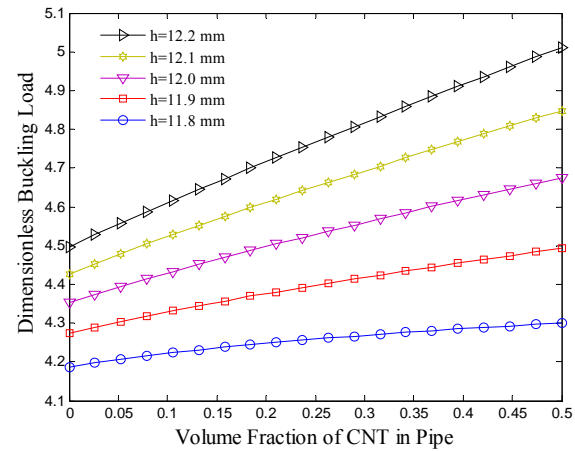

Fig. 3   The effect of temperature change on the dimensionless buckling load versus volume percent of CNTs in sea lines
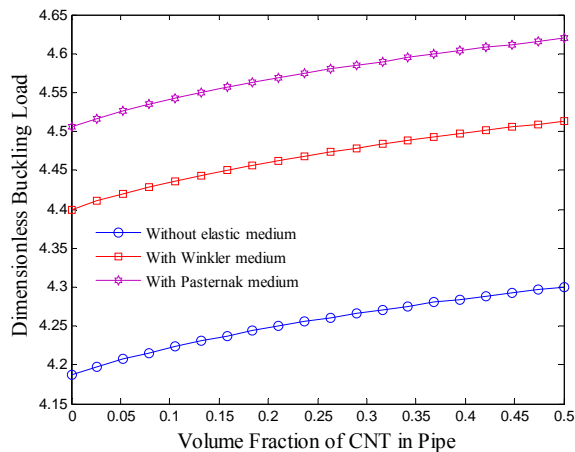
Fig. 4 illustrates the influence of the Poisson's ratio on the dimensionless buckling load versus volume percent of CNTs in sea lines. As can be seen, the dimensionless buckling load increases with increasing Poisson's ratio.
Fig. 5 shows the influence of elastic medium, including Winkler and Pasternak modules, the dimensionless buckling load versus volume percent of CNTs in sea lines. It can be concluded that the higher the Winkler and Pasternak constants, the higher dimensionless buckling load. This is perhaps because increasing Winkler and Pasternak coefficient increases the pipe stiffness. It is also worth to mention that the dimensionless buckling load for Pasternak medium is higher than Winkler medium.
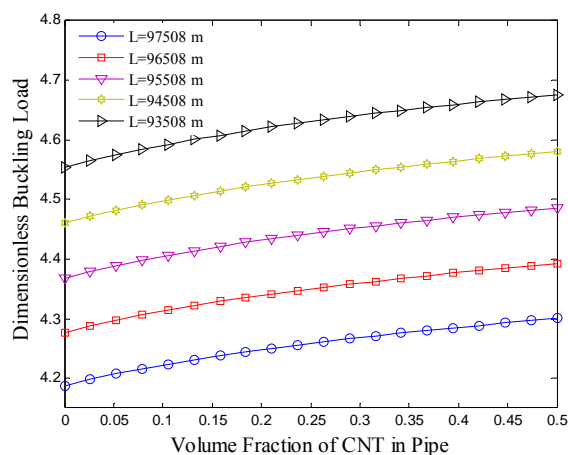
Fig. 4 The effect of Poisson's ratio on the dimensionless buckling load versus volume percent of CNTs in sea lines

Fig. 5 The effect of elastic medium on the dimensionless buckling load versus volume percent of CNTs in sea lines

Fig. 6 The effect of pipe length on the dimensionless buckling load versus volume percent of CNTs in sea lines

Fig. 7 The effect of thickness pipe on the dimensionless buckling load versus volume percent of CNTs in sea lines

It is due to the fact that Pasternak medium suggested considering not only the normal stresses but also the transverse shear deformation and continuity among the spring elements, and its subsequent applications for developing the model for buckling analysis proved to be more accurate than Winkler model.

The effects of geometrical parameters including length and thickness of the sea lines on the dimensionless buckling load versus volume percent of CNTs in sea lines are demonstrated in Figs. 6 and 7. It can be observed that the dimensionless buckling load decreases with increasing length and thickness of the sea lines. It is because with increasing length and thickness of the sea lines, the stability and stiffness of the system decreases.

7   CONCLUSION

The main contribution of the present study was the effect of CNT on the buckling of the sea lines embedded in Pasternak foundation. The sea lines were simulated with cylindrical shell and were reinforced by CNTs. The characteristics of the equivalent nanocomposite were determined using Mori-Tanaka model.

Based on energy method and Hamilton's principal, the governing equations are derived so that the effects of volume percent of CNTs in sea lines, geometrical parameters, elastic medium constants, temperature change and poison ratio on the buckling load of the system are studied. Results indicate that the dimensionless buckling load increases with increasing volume percent of CNTs. It was found that the higher the Winkler and Pasternak constants, the higher the dimensionless buckling load. Furthermore, the

dimensionless buckling load decreases with increasing length and thickness of the sea lines.Finally, it is hoped that the results proposed in this investigation would be helpful for the design of the oil pipes in sea lines.

ACKNOWLEDGMENT

I should thank pars oil & gas Company for having sponsored this project.

REFERENCES

[1] Merhari Hybrid, L., "Nanocomposites for nanotechnology", Springer Science, New York, 2009.

[2] Schwartz, M., "SMART MATERIALS", John Wiley and Sons, A Wiley-Interscience Publication Inc., New York, 2002.

[3] Kotsilkova, R., "Thermoset nanocomposites for engineering applications", Smithers Rapra Technology, USA, 2007.

[4] Yu, V., Christopher, T., and Bowen, R., "Electromechanical properties in composites based on ferroelectrics", Springer-Verlag, London, 2009.

[5] Vang, J., "The mechanics of piezoelectric structures", World Scientific Publishing Co., USA, 2006.

[6] Brockmann, T. H., "Theory of adaptive fiber composites from piezoelectric material behaviour to dynamics of rotating structures", Solid Mech.Its Appl., USA, 2009.

[7] Karam, G. N., Gibson, L.J., "Elastic buckling of cylindrical shells with elastic cores I. analysis", International Journal of Solids and Structures, Vol. 32, 1995, pp. 1259-1283.

[8] Agarwal, B. L., Sobel, L.H., "Weight comparisons of optimized stiffened, unstiffened, and sandwich cylindrical shells", AIAA Journal, Vol. 14, 1977, pp. 1000-1008.

[9] Hutchinson, J. W., He, M. Y., "Buckling of cylindrical sandwich shells with metal foam cores", Vol. 37, 2000, pp. 6777-6794.

[10] Ghorbanpour Arani, A., Golabi, S., Loghman, A., and Daneshi, H., "Investigating elastic stability of cylindrical shell with an elastic core under axial compression by energy method", Journal of Mechanical Science and Technology, Vol. 21, 2007, pp. 693-698.

[11] Ye, L., Lun, G., and Ong, L. S., "Buckling of a thin-walled cylindrical shell with foam core under axial compression", Thin-Walled Structures, Vol. 49, 2011, pp. 106-111.

[12] Ray, M. C., Reddy, J. N., "Active control of laminated cylindrical shells using piezoelectric fiber reinforced composites," Composite Science and Technology, Vol. 65, 2005, pp. 1226-1236.

[13] Bohm, H. J., Nogales, S., "Mori–Tanaka models for the thermal conductivity of composites with interfacial resistance and particle size distributions", Composite Science and Technology, Vol. 68, 2008, pp. 1181-1187.

[14] Wan, H., Delale, F., and Shen, L., "Effect of CNT length and CNT-matrix interphase in carbon nanotube (CNT) reinforced composites", Mechanics Research Communications, Vol. 3, 2005, pp. 481-489.

[15] Shi, D. L., Feng, X. Q., Huang, Y. Y., Hwang, K. C., and Gao, H.,"The Effect of nanotube waviness and agglomeration on the elastic property of carbon nanotube-reinforced composites", Journal of Engineering Mechanics, Vol. 126, 2004, pp. 250-257.

[16] Kollar, L. P., Springer, G. S., "Mechanics of Composite Structures", Cambridge University Press NY, USA, 2003.

APPENDIX A

$$h_s C_{s11}\left(\frac{\partial^2 u}{\partial x^2}+\frac{\partial w}{\partial x}\frac{\partial^2 w}{\partial x^2}\right)+\frac{h_s C_{s12}}{R_s}\left(\begin{array}{c}\frac{\partial^2 v}{\partial x\partial\theta}+\frac{\partial w}{\partial x}\\+\frac{\partial w}{R_s\partial\theta}\frac{\partial^2 w}{\partial x\partial\theta}\end{array}\right)$$

$$+\frac{h_s C_{s66}}{R_s}\left(\begin{array}{c}\frac{\partial^2 u}{R_s\partial\theta^2}+\frac{\partial^2 v}{\partial x\partial\theta}+\frac{\partial w}{R_s\partial x}\frac{\partial^2 w}{\partial\theta^2}\\+\frac{\partial w}{\partial x}+\frac{\partial w}{R_s\partial\theta}\frac{\partial^2 w}{\partial x\partial\theta}\end{array}\right)=0, \tag{A1}$$

$$\frac{h_s C_{s12}}{R_s}\left(\frac{\partial^2 u}{\partial x\partial\theta}+\frac{\partial w}{\partial x}\frac{\partial^2 w}{\partial x\partial\theta}\right)+\frac{h_s C_{s22}}{R_s^2}\left(\begin{array}{c}\frac{\partial^2 v}{\partial\theta^2}+\frac{\partial w}{\partial\theta}\\+\frac{\partial w}{R_s\partial\theta}\frac{\partial^2 w}{\partial\theta^2}\end{array}\right)$$

$$+h_s C_{s66}\left(\begin{array}{c}\frac{\partial^2 u}{R_s\partial x\partial\theta}+\frac{\partial^2 v}{\partial x^2}+\\\frac{\partial^2 w}{R_s\partial\theta\partial x}\frac{\partial w}{\partial x}+\frac{\partial w}{R_s\partial\theta}\frac{\partial^2 w}{\partial x^2}\end{array}\right)=0, \tag{A2}$$

$$\frac{h_s^3}{12}\left(-C_{s11}\frac{\partial^4 w}{\partial x^4}-\frac{2C_{s12}}{R_s^2}\frac{\partial^4 w}{\partial x^2\partial\theta^2}-\frac{C_{s22}}{R_s^4}\frac{\partial^4 w}{\partial\theta^4}\right)$$

$$-\frac{h_s^3 C_{c66}}{3R_s^2}\left(\frac{\partial^4 w}{\partial x^2\partial\theta^2}\right)-\frac{h_s C_{s12}}{R_s}\left(\frac{\partial u}{\partial x}+\frac{1}{2}\left(\frac{\partial w}{\partial x}\right)^2\right)$$

$$-\frac{h_s C_{s22}}{R_s}\left(\frac{\partial v}{\partial\theta}+\frac{w}{R_s}+\frac{1}{2R_s^2}\left(\frac{\partial w}{\partial\theta}\right)^2\right)$$

$$-\left(\frac{h_s C_{s22}\alpha_{xs}}{R_s}+\frac{h_s C_{s12}\alpha_{\theta s}}{R_s}\right)\frac{\partial^2 w}{\partial\theta^2}\Delta T \tag{A3}$$

$$-\left(h_s C_{s11}\alpha_{xs}+h_s C_{s12}\alpha_{\theta s}\right)\frac{\partial^2 w}{\partial x^2}\Delta T$$

$$+N_x\frac{\partial^2 w}{\partial x^2}+\left(k_w w_1-k_g\left(\frac{\partial^2 w}{\partial x^2}+\frac{\partial^2 w}{R_s\partial\theta^2}\right)\right)=0.$$